A Novel Total Variation Based Noninvasive Transmural Electrophysiological Imaging

Jingjia Xu, Azar Rahimi Dehaghani , Fei Gao, and Linwei Wang

Computational Biomedicine Laboratory, Golisano College of Computing and Information Sciences, Rochester Institute of Technology, Rochester, NY, 14623, USA

Abstract. While tomographic imaging of cardiac structure and kinetics has improved substantially, electrophysiological mapping of the heart is still restricted to the body or heart surface with little or no depth information beneath. The progress in reconstructing transmural action potentials from surface voltage data has been hindered by the challenges of intrinsic ill-posedness and the lack of a unique solution in the absence of prior assumptions. In this work, we propose to exploit the unique spatial property of transmural action potentials that it is often piecewise smooth with a steep boundary (gradient) separating the depolarized and repolarized regions. This steep gradient could reveal normal or disrupted electrical propagation wavefronts, or pinpoint the border between viable and necrotic tissue. In this light, we propose a novel adaption of the total-variation (TV) prior into the reconstruction of transmural action potentials, where a variational TV operator is defined instead of a common discrete operator, and the TV-minimization is solved by a sequence of weighted, first-order L2-norm minimizations. In a large set of phantom experiments performed on image-derived human heart-torso models, the proposed method is shown to outperform existing quadratic methods in preserving the steep gradient of action potentials along the border of infarcts, as well as in capturing the disruption to the normal path of electrical wavefronts. The former is further attested by real-data experiments on two post-infarction human subjects, demonstrating the potential of the proposed method in revealing the location and shape of the underlying infarcts when existing quadratic methods fail to do so.

Keywords: Electrophysiological imaging, inverse problems, total-variation.

1 Introduction

The heart is an electromechanical organ. Its efficient contraction must be coordinated by a steady electrical flow spreading three-dimensionally throughout the myocardium. Disruptions to this electrical propagation can directly predispose the heart to mechanical catastrophe and lead to sudden cardiac death. However, while methods for noninvasive imaging and analysis of 3D structure, kinetics, and mechanics of an individual's heart have substantially improved in recently years, methods for assessing the electrophysiological (EP) aspects have

K. Mori et al. (Eds.): MICCAI 2013, Part I, LNCS 8149, pp. 501–508, 2013.

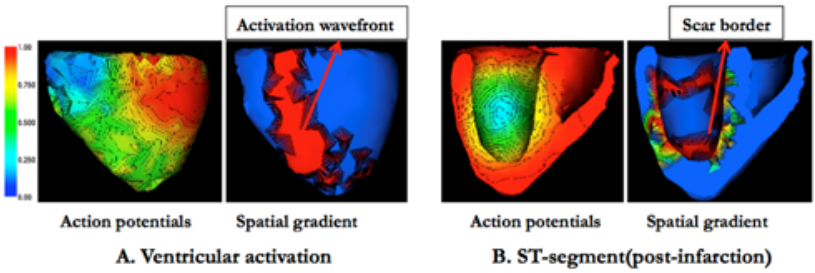

Fig. 1. Illustration of the transmural action potential and its spatial gradient

not. In practice, common observations of cardiac electrical activities are voltage data either sensed on the body-surface as noninvasive electrocardiograms (ECG), or mapped on heart surfaces by catheters introduced into the cavity in a minimally-invasive manner. Both data provide a poor surface surrogate for intramural electrical activities that occur deep beneath the surface of the heart.

The critical gap in experimental methods has motivated many computational methods for *EP imaging* that, analogous to tomographic imaging, solve an inverse problem to quantitatively reconstruct transmural action potentials from body-surface voltage data, the forward relationship of which is governed by the *quasi-static electromagneticism* [8]. Unfortunately, in addition to mathematic ill-posed caused by limited number of data that is common to many inverse problems, this biophysical principle determines that there may be an infinite number of solutions that fit the same surface measurement [8]. For a unique solution, a common assumption restricts to the surface of the heart [9]. This guarantees a unique surface solution as a surrogate for the intramural electrical dynamics, and various regularization methods have been applied to reduce the mathematical ill-posedness. Transition to intramural EP imaging has been very limited, and existing methods [7,13] again all essentially amount to a weighted quadratic regularization that imposes either the spatial and/or temporal smoothness of the solution or the conforming to a complex physiological prior [14]. Due to the heuristic model of smoothness, these solutions are observed to be diffused and lose sharp details that are physiologically and clinically critical [14,13].

Our fundamental hypothesis is that, while quadratic methods are suitable for alleviating the mathematical ill-posedness of this problem caused by limited data, sparse methods are further needed for the physically-included non-uniqueness of solutions. In particular, we propose a fresh perspective to view the transmural action potential $u(t)$ as a time-varying 3D image. As illustrated in Fig 1, the edge of this image (*i.e.*, spatial gradient $\nabla u(t)$) is always localized and steep in space. During the depolarization and repolarization, it represents the steep *wavefront* between active and resting regions (Fig. 1 A), revealing potential disruptions to the path of normal electrical flow in diseased hearts. Between the two phases (the ST-segment of an ECG cycle), $\nabla u(t)$ is expected to be close to zero everywhere in a normal heart and appearance of high gradient would again indicate underlying diseases, such as the border of an infarct that divides

regions of depolarized viable tissue and necrotic infarct core (Fig. 1 B). This unfolds the importance to preserve the unique spatial feature of $\nabla u(t)$ during the reconstruction of $u(t)$, which is in line with the essence of total-variation (TV) minimization to promote a solution with sharp boundaries/gradients between piecewise smooth regions. Since its original development, TV minimization has been applied to preserve the sharp edge of an image in a variety of applications such as image de-noising [11] and blind de-convolution [2].

In this paper, we propose a novel adaptation of the spatial TV-prior into transmural EP imaging. We first define a variational form of TV-prior to approximate the continuous TV form by a numerical integration, so as to overcome the weakness of a common discrete TV-prior in being error-prone to calculate on the irregular mesh of the heart. The concept of iteratively re-weighted norm (IRN) method is then coupled with this TV-prior to solve the TV minimization. In a set of 137 phantom experiments, the proposed method was shown to deliver significantly higher accuracy (paired t-test) over existing quadratic methods in preserving the steep gradient of action potentials that is distributed along the border of an infarct during the ST-segment. It is also shown to outperform existing quadratic methods in preserving the structure of electrical propagation wavefronts, and in capturing the change of these wavefronts caused by the existence of an infarct. Real-data experiments on two post-infarction patients further verify the potential of the proposed method in detecting the abnormally steep gradient and thus revealing the shape of the infarct border.

2 Methodology

Cardiac electrical flow produces time-varying voltage data, easily accessible on the body-surface, as if our torso were a *quasi-static* electromagnetic field [8]. With different numerical methods and discrete representation of the heart-torso anatomy of a given subject [7,14], this biophysical relationship can be represented in a matrix form: $\phi(t) = \mathbf{H}\mathbf{u}(\mathbf{t})$, where $\phi(t)$ is the discrete field of voltage data sensed on the body surface, $\mathbf{u}(t)$ the discrete filed of transmural action potential across the depth of the myocardium, and the transfer matrix $\mathbf{H}$ is specific to each individual's torso anatomy and typically considered time-invariant. The condition number of $\mathbf{H}$ was shown to be typically at the order of 10^{-14} [14]. We propose to incorporate the TV-prior into the reconstruction of transmural action potentials and, at this stage, we exclude the temporal factor and focus on the reconstruction with a spatial TV-prior at separate time instants:

$$\hat{\mathbf{u}} = \min_{\mathbf{u}}\{||\mathbf{H}\mathbf{u} - \phi||_2^2 + \lambda TV(\mathbf{u})\} \tag{1}$$

Variational TV-form: The first challenge comes from the need of a proper definition of $TV(\mathbf{u})$. In image-processing applications, a discrete version of $TV(\mathbf{u})$ is calculated as the *L1-norm of the discrete gradient field of* $\mathbf{u}$: $TV(\mathbf{u}) = ||\nabla\mathbf{u}||_1 = \sum_{i=1}^{n}\sqrt{\nabla_x\mathbf{u}_i^2 + \nabla_y\mathbf{u}_i^2 + \nabla_z\mathbf{u}_i^2}$. However, it is not possible to formulate an explicit gradient operator for the entire discrete field without separately employing directional gradient operators. Furthermore, the gradient field is highly affected

by the resolution of the discrete field $\mathbf{u}$, and is much more difficult and error-prone to calculate on the complex mesh of the heart than a regular image. Therefore, we define an approximation of the continuous form of TV as:

$$TV(\mathbf{u}) = \int_{\Omega_h} |\nabla u| d\Omega_h \approx \Sigma_{i=1}^{N} |\nabla \varphi_i \mathbf{u}| \tag{2}$$

where a numerical integration is performed over the myocardial field Ω_h, involving a summation of ∇u over N (at the order of 10^5) Gaussian quadrature points. Based on the discretization method used (meshfree method used in our study), ∇u on each Gauss point is approximated by a linear combination of its neighboring points in the discrete field $\mathbf{u}$ based on the $1 \times n$ shape functions φ_i ($\nabla \varphi_i$ being the $3 \times n$ spatial gradients of φ_i). Because each Gauss point has a small set of support nodal points, φ_i and $\nabla \varphi_i$ are sparse with a small number of non-zero values. This definition of $TV(\mathbf{u})$ is also consistent with the data-fidelity term in equation (1), where the biophysical model $\mathbf{H}$ is calculated from numerical approximations of integrals involved in the *quasi-static* Maxwell equations.

TV-minimization with Iteratively Re-weighted Norm (TVIRN): To solve the L1-norm penalty function in equation (1), we adopt the concept of IRN [10], so that variational form of TV (2) is approximated as a sequence of L2 norm of the weighted gradient; each weight is the square root of the gradient value in the previous $(k-1)$-th iteration for $k = 1, 2, \cdots$ until convergence. In this way, a small spatial gradient in previous iterations will generate a large penalty in the current iteration, while a large gradient will be promoted until the final solution exhibits a piecewise smooth pattern with steep gradient in between:

$$\int_{\Omega_h} |\nabla u^{(k)}| d\Omega_h \approx \int_{\Omega_h} |\frac{\nabla u^{(k)}}{\sqrt{\nabla u^{(k-1)}|}}|^2 d\Omega_h \approx \mathbf{u}^{(k)^T} (\sum_{i=1}^{N} \frac{(\nabla \varphi_i^T \nabla \varphi_i)}{|\nabla \varphi_i \mathbf{u}^{(k-1)}|}) \mathbf{u}^{(k)} \tag{3}$$

The weight matrix is calculated over N Gaussian quadrature points. Each sparse matrix $\nabla \varphi_i^T \nabla \varphi_i$ on each Gauss point is constant once the discretization of the ventricular model is established and only needs to be computed once for the entire recursive procedure. At each iteration, it is weighted by action potential of the same Gauss point $|\nabla \varphi_i \mathbf{u}^{(k-1)}|$ calculated from $\mathbf{u}^{(k-1)}$. Therefore, the TV-minimization (1) can be solved by a set of weighted L2-minimizations:

$$\hat{\mathbf{u}}^{(k)} = \min_{\mathbf{u}} ||\mathbf{H}\mathbf{u}^{(k)} - \phi||_2^2 + \lambda^{(k)} \mathbf{u}^{(k)^T} (\sum_{i=1}^{N} \frac{(\nabla \varphi_i^T \nabla \varphi_i)}{|\nabla \varphi_i u^{(k-1)}|}) \mathbf{u}^{(k)} \tag{4}$$

$$\rightarrow \hat{\mathbf{u}}^{(k)} = (\mathbf{H}^T \mathbf{H} + \lambda^{(k)} \sum_{i=1}^{N} \frac{\nabla \varphi_i^T \nabla \varphi_i}{|\nabla \varphi_i \mathbf{u}^{(k-1)}| + \beta})^{-1} \mathbf{H}^T \phi \tag{5}$$

where $\lambda^{(k)}$ is the regularization parameter used at iteration k. β is a small positive value to reduce numerical errors when $|\nabla \varphi_i \mathbf{u}^{(k-1)}|$ at the i-th Gauss point is close to zero. As explained above, at each iteration the optimization (5) involves only a weighted summation of the set of N pre-stored matrices, and the matrix inversion is calculated by *Conjugate Gradient* method in this study.

Algorithm 1. Total-Variation Iteratively Re-weighted Norm (TVIRN)

Initialization: $\mathbf{u}^{(0)} = (\mathbf{H}^T\mathbf{H} + \lambda_0\mathbf{W}^T\mathbf{W})^{-1}\mathbf{H}^T\mathbf{\Phi}$, $k = 1$
while $(||TV(\mathbf{u}^{(k)}) - TV(\mathbf{u}^{(k-1)})||_2 \leq tol$, tol $= 10^{-5})$
$\lambda^{(k)} = \frac{||\mathbf{H}^T\mathbf{H}||_\infty}{||\sum_{i=1}^{N} \frac{\nabla\varphi_i^T\nabla\varphi_i}{|\nabla\varphi_i\mathbf{u}^{(k-1)}|+\beta}||_\infty}$, $\hat{\mathbf{u}}^{(k)} = (\mathbf{H}^T\mathbf{H} + \lambda^{(k)}\sum_{i=1}^{N} \frac{\nabla\varphi_i^T\nabla\varphi_i}{|\nabla\varphi_i\mathbf{u}^{(k-1)}|+\beta})^{-1}\mathbf{H}^T\mathbf{\Phi}$
$k = k + 1$
end

Algorithm Summary: A summary of the algorithm is provided in Algorithm 1. First, an existing weighted quadratic method [7] is used to overcome the mathematical ill-posedness of the problem and to obtain an initial solution of $\mathbf{u}^{(0)}$. The regularization parameter $\lambda^{(0)}$ is calculated by the L-curve method [5]. After initialization, the iteration as described above (5) repeats until the convergence criterion, *i.e.*, the difference between two successive gradients of solutions is smaller than a pre-defined tolerance. There is currently no established method for determining regularization parameter in L1-based problems, and most works rely on an empirical procedure to select an optimal value of λ after a large set of experiments. Here we use a more objective method [12] to automatically update the magnitude of $\lambda^{(k)}$ at each iteration based on the infinity norm of the matrices involved in the data-fidelity and the regularization terms (see Algorithm 1).

3 Experiments and Results

Phantom and real-data experiments are both used in this study. Phantom experiments are conducted on four realistic human heart-torso models derived from CT images, where we test the proposed method in preserving: 1) steep $\nabla\mathbf{u}$ along the border of infarcts during the ST-segment, and 2) propagation wavefronts in normal versus infarcted hearts. Two real-data experiments are further performed on post-infarction human subjects to detect the steep gradient of action potentials distributed along the border of infarcts. The accuracy is measured by the *consistency metric* $CoM = \frac{S_1 \cap S_2}{S_1 \cup S_2}$ between the region of steep gradients (S_1) in reconstructed action potentials and the *true* region of steep gradients(S_2). In current study, a threshold value is automatically calculated from the mean and standard deviation of result. Comparison studies are performed between TVIRN and existing quadratic methods for transmural EP imaging, including the 1-order [13] and 0-order [7] Tikhonov regularization.

Steep Potential Gradients Along Infarct Border: In this set of phantom experiments, action potentials during the ST-segment are set to be 0 for the infarct core, and 1 for the health region(normalized physiological range(-20-90)). 370-lead or 120-lead body-surface ECG are simulated and corrupted with 20-dB Gaussian noise as inputs for transmural *EP imaging*. We consider infarcts of different sizes and locations according to the 17 standard AHA segments of LV. In total we consider 137 cases of infarcts of different locations and sizes from 0.5% to 50% of LV. On average the TVIRN takes 8.5 iterations to converge.

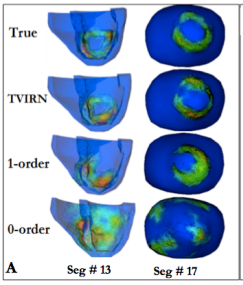

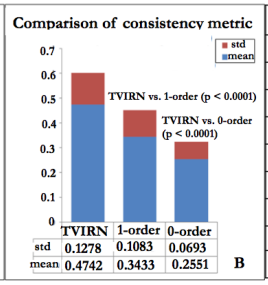

C	TVIRN	1-order	0-order
ANT (26)	0.51±0.10	0.36±0.07	0.24±0.06
INF (21)	0.49±0.07	0.32±0.07	0.24±0.05
LAT (40)	0.54±0.11	0.40±0.10	0.29±0.08
SEP (29)	0.34±0.09	0.27±0.12	0.23±0.07
APX (4)	0.61±0.13	0.47±0.17	0.18±0.09
0-5%(29)	0.51±0.10	0.33±0.12	0.22±0.07
5-10%(31)	0.47±0.14	0.34±0.11	0.27±0.09
10-20%(49)	0.48±0.13	0.35±0.11	0.26±0.07
>20%(28)	0.43±0.11	0.35±0.09	0.25±0.04

Fig. 2. Reconstruction accuracy in preserving the steep gradient of transmural action potentials during the ST-segment of an ECG cycle in infarcted hearts. A. Two examples of steep action potential gradients along the infarcts. B and C. Quantitative analysis.

Fig 2 (A) shows two examples of the *true* steep spatial gradients of action potentials along border of infarcts located at anterior (segment 13) and apical (segment 17) regions of the LV, respectively. This spatial structure of the steep gradient is well preserved in the reconstructed action potentials by TVIRN method. In comparison, gradient of the action potential reconstructed by the 0-order quadratic method is diffused and does not reveal the location or the shape of the underlying infarcts. The 1-order quadratic regularization shows improved accuracy over its 0-order counterpart but the reconstructed gradient is still blurred and loses the topology of the infarct border.

Fig 2 (B) lists the *consistency metric* for 137 cases, where paired student's t-test shows that the accuracy of TVIRN at the steep action potential gradients is significantly higher than that of the other two quadratic methods ($p < 0.0001$). Fig 2 (C) lists the *COM* with respect to the locations and sizes of the infarcts, respectively. As shown, TVIRN has the best performance when the infarcts are located at apical and lateral regions of the heart. It is the most difficult to correctly capture the gradient of action potentials when the infarct is at the septal area of the LV, the region most hidden from body-surface data. The accuracy of TVIRN is similar dealing with infarcts of different sizes.

Activation/repolarization Wavefronts: We continue to consider whether TVIRN can capture disruptions to electrical propagation wavefronts (steep gradient of action potentials) caused by the existence of infarcts. In this set of experiments, transmural propagation of ventricular action potentials is simulated with the *Aliev-Panfilov* model [1] with parameter a (representing tissue excitability) set to be 0.5 for infarcts and 0.15 for healthy tissue. Time sequences of 120-lead ECGs are simulated and corrupted with 20-db white Gaussian noise. Selected time frames during activation or repolarization are used for reconstructions.

Depolarization: Fig 3 (A,C) shows an example of the activation wavefront in a normal heart when the electrical flow propagates from the RV to LV (purple arrow), and that at the same time instant on the same heart model but with an infarct localized at the mid-basal anterior region of the LV (labeled by red line). It is evident that the infarct works as a structural obstacle and re-routes

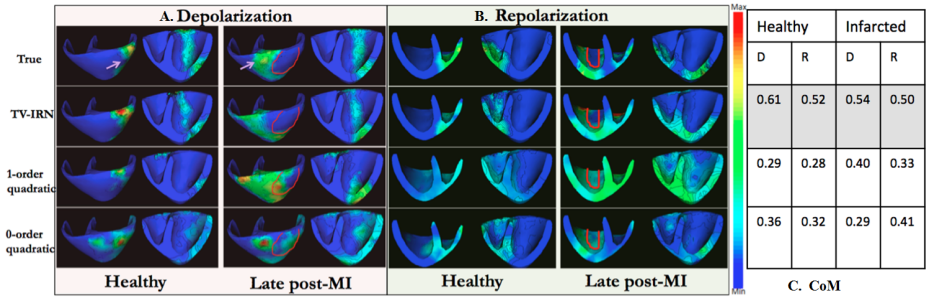

	Healthy		Infarcted	
	D	R	D	R
True	0.61	0.52	0.54	0.50
TV-IRN	0.29	0.28	0.40	0.33
1-order quadratic	0.36	0.32	0.29	0.41
0-order quadratic				

Fig. 3. Change of propagation wavefronts in normal and infarcted hearts. The proposed TVIRN faithfully captures the change of path while quadratic methods fail to do so.

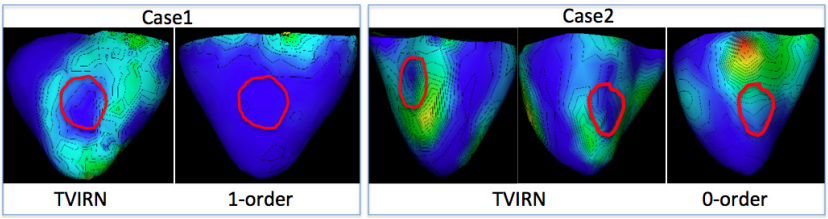

Fig. 4. Spatial gradients of transmural action potentials reconstructed from TVIRN and quadratic methods on two post-infarction human hearts. The red cycles represent the core of the MRI-delineated infarcts.

the activation wavefront. The proposed method captures the steep wavefront in the reconstructed action potential in both normal and disrupted electrical flow. In comparison, the 0-order quadratic method fails to distinguish the depolarized region from the resting region in both cases. The 1-order quadratic method partially captures the wavefront but not on the endocardium, and it also fails to accurately reflect the disruption caused by the infarct.

Repolarization: Fig 3 (B,C) shows the repolarization wavefront of the same normal and infarcted hearts, where the infarct both disrupts the repolarization wavefront and changes the action potential gradients around the infarct border. Again, TVIRN method is able to capture both the normal and disrupted spatial gradients of the reconstructed action potentials. In comparison, the other two quadratic methods fail to reveal the abnormal repolarlzation wavefront related to the location or structure of the infarct.

Real-data Study of Steep Gradient Along Infarct Border: We consider MRI and body-surface ECG data on two post-infarction patients made available to this study by the *2007 PhysioNet / Computers in Cardiology Challenges* [4]. MRI data are used to construct the patient-specific heart-torso model. Body-surface ECG data were recorded by standard 120-lead Dalhousie protocol [6]. Gold standards of infarct quantification were obtained form Gadolinium-enhanced MRI by cardiologists, revealing that the core regions of the infarct are labeled by the red cycle in Fig 4. As shown in Fig 4, both of reconstructed

action potentials of TVIRN exhibit a steep gradient that are localized and distributed along the infarct cores, even in case 2 with two separate infarct regions. In comparison, action potentials reconstructed from neither of the other two quadratic methods reveal any physiological meaningful information regarding the existence, location, or structure of the infarct. These observations are consistent with the findings in our phantom experiments.

Conclusion: This paper presents a novel approach to transmural EP imaging based on a spatial TV-prior, and demonstrates its superiority over existing quadratic methods in a set of phantom and real-data experiments. The adaption of TV-prior was also recently considered for potential reconstruction on the epicardium [3]. In comparison, our method is first proposed to reconstruct transmural action potential with a close tie its spatial property. The next immediate step is to integrate temporal constraints with the spatial TV-prior to improve the accuracy and temporal consistency of the proposed method.

References

1. Aliev, R.R., et al.: A simple two-variable model of cardiac excitation. Chaos, Solitions & Fractals 7(3), 293–301 (1996)
2. Chan, T., Wong, C.K.: Total variation blind deconvolution. IEEE Transactions on Image Processing 7(3), 370–375 (1998)
3. Ghosh, S., Rudy, Y.: Application of l1-norm regularization to epicardial potential solutions of the inverse electrocardiography problem. Annals of Biomedical Engineering 37(5), 902–912 (2009)
4. Goldberger, A.L., et al.: Physiobank, physiotoolkit, and physionet: Components of a new research resource for complex physiological signals. Circulation 101, e215–e220 (2000)
5. Hansen, P., O'Leary, D.: The use of the l-curve in the regularization of discrete ill-posed problems. SIAM Journal on Scientific Computing 14(6), 1487–1503 (1993)
6. Hubley-Kozey, C.L., Mitchell, L.B., Gardner, M.J., et al.:
7. Liu, Z., Liu, C., He, B.: Noninvasive reconstruction of three-dimensional ventricular activation sequence from the inverse solution of distributed equivalent current density. IEEE Transactions on Medical Imaging 25(10), 1307–1318 (2006)
8. Plonsey, R.: Bioelectric phenomena. Wiley Online Library (1999)
9. Ramanathan, C., Ghanem, R., et al.: Noninvasive electrocardiographic imaging for cardiac electrophysiology and arrhythmia. Nature Medicine 10(4), 422–428 (2004)
10. Rodríguez, P., Wohlberg, B.: Efficient minimization method for a generalized total variation functional. IEEE Transactions on Image Processing 18(2), 322–332 (2009)
11. Rudin, L., Osher, S., Fatemi, E.: Nonlinear total variation based noise removal algorithms. Physica D 60, 259–268 (1992)
12. Schmidt, M., Fung, G., Rosales, R.: Optimization methods for l1-regularization. University of British Columbia, Technical Report TR-2009-19 (2009)
13. Wang, D., Kirby, R., MacLeod, R., Johnson, C.: Identifying myocardial ischemia by inversely computing transmembrane potentials from body-surface potential maps. In: International Symposium on NFSIBH, pp. 121–125 (2011)
14. Wang, L., Wong, K., Zhang, H., Liu, H., Shi, P.: Noninvasive computational imaging of cardiac electrophysiology for 3-d infarct. IEEE Transactions on Biomedical Engineering 58(4), 1033–1043 (2011)